Supporting Information

Fitzpatrick et al. 10.1073/pnas.1502214112

SI Methods

Ring Fitting. In the cases of an ensemble of crystals and a fibril network, the diffraction pattern consists of Debye–Scherrer rings. The center of the diffraction rings in each pattern is determined by a Hough transform as used in image theory, allowing us to compensate for any drift of the electron beam due to transient electric fields (1). Azimuthal averaging of the pattern gives the diffraction intensity as a function of the scattering vector, s (rocking curve). The peaks are indexed on the basis of the monoclinic unit cell. For data analysis, the rocking curve is decomposed into background and diffraction peaks. A least-square fitting allows us to determine the position and the intensity change of every peak as a function of the delay time between photon–pump and electron–probe.

For the case of an ensemble of crystals, the observed rocking curve is decomposed into several peaks. The absence of correlation between their positions, as obtained from the fitting procedure, is verified by evaluating the covariance matrix, from which a Pearson's coefficient, p, of 0.1 is obtained (complete correlation would be present if p is 1 or −1).

Determination of Temperature Jump. In the framework of an equilibrium heating model (2) the laser irradiation is able to induce a temperature increase, ΔT, within the investigated material. The thermal motions excited by this temperature jump are responsible for a loss of interference within the lattice, which results in a reduction of the diffraction intensity, quantitatively described by the Debye–Waller relation:

$$\ln\left(\frac{I_0}{I}\right) = 2\left[W(T,\Theta_D) - W(T_0,\Theta_D)\right],$$

where $T = T_0 + \Delta T$, Θ_D is the Debye temperature, W is the Debye–Waller factor, and I_0 and I are the diffraction intensities before and after the optical excitation, respectively. The Debye–Waller factor can be expressed as

$$W(T,\Theta_D) = \frac{3\hbar^2 s^2}{2MK_B\Theta_D}\left[\frac{1}{4} + \left(\frac{T}{\Theta_D}\right)^2 \int_0^{\Theta_D/T} \frac{\mu}{\exp(\mu)-1}d\mu\right],$$

where M is the average atomic mass, K_B is the Boltzmann constant, and $\hbar$ is the Planck constant.

For the case of protein fibrils discussed in this work, the value of the temperature increase, ΔT, can be extracted by the Debye–Waller relation using the experimentally measured value of intensity change for the diffraction peak at 4.8 Å and a Debye temperature $\Theta_D = 100$ K (3).

Dipole–Dipole Interactions Between Amyloid Protofilaments. By analogy with microtubules (4), the force of electrostatic attraction arising from dipole–dipole interactions between neighboring protofilaments, $F_{electrostatic}$, is given by

$$F_{electrostatic} \approx \frac{a^3\sigma_D^2 d^2\pi}{\varepsilon_0\varepsilon\lambda^2\sqrt{d^2+a^2}(d^2+2a^2)^2} \times\left\{\frac{3}{8}\frac{L}{\sqrt{d^2+2a^2}}\tan^{-1}\left(\frac{L}{\sqrt{d^2+2a^2}}\right) + \frac{1}{8}\sin^2\left[\tan^{-1}\left(\frac{L}{\sqrt{d^2+2a^2}}\right)\right]\right\},$$

where a is the protofilament radius [22 Å for VQIVYK (5)], d is the distance between protofilaments, σ_D is the dipole moment per unit area (7.9×10^{-11} C/m for VQIVYK), λ is a constant (~2–3), ε is the dielectric constant of water, and L is the length of the fibril [typically between 1 and 3 μm (6)]. The bond stiffness, $k_{electrostatic}$, is calculated as $k_{electrostatic} = [dF_{electrostatic}/dd]_{d\,=\,2a}$.

Effective Bending Rigidity of Individual Amyloid Fibrils. By analogy with cytoskeletal bundle mechanics (7), the effective bending rigidity, κ_B, is given by

$$\kappa_B = \kappa_f N\left(1 + \frac{\chi^2(N-1)}{1 + c\dfrac{N+\sqrt{N}}{\gamma}}\right),$$

where κ_f is the bending stiffness of a single β-sheet (~1×10^{-26} N m^2), N is the total number of intersheet and interprotofilament interfaces per 4.8 Å layer of fibril, χ and c are constants (7), and γ is the protofilament coupling parameter, as described in the main text.

1. Schäfer S, Liang W, Zewail AH (2010) Structural dynamics and transient electric-field effects in ultrafast electron diffraction from surfaces. *Chem Phys Lett* 493:11–18.
2. Schäfer S, Liang W, Zewail AH (2011) Primary structural dynamics in graphite. *New J Phys* 13:063030.
3. Frauenfelder H, Chan SS, Chan WS, eds (2010) *An Introduction to Biological Physics and Molecular Biophysics* (Springer, New York).
4. Tuszyński JA, et al. (2005) Molecular dynamics simulations of tubulin structure and calculations of electrostatic properties of microtubules. *Math Comput Model* 41: 1055–1070.
5. Landau M, et al. (2011) Towards a pharmacophore for amyloid. *PLoS Biol* 9(6):e1001080.
6. Fitzpatrick AWP, et al. (2013) Atomic structure and hierarchical assembly of a cross-β amyloid fibril. *Proc Natl Acad Sci USA* 110(14):5468–5473.
7. Bathe M, Heussinger C, Claessens MMAE, Bausch AR, Frey E (2008) Cytoskeletal bundle mechanics. *Biophys J* 94(8):2955–2964.

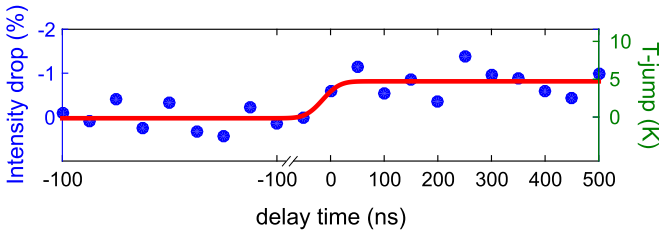

Fig. S1. Representative intensity drop/temperature jump curve for amyloid fibril networks.

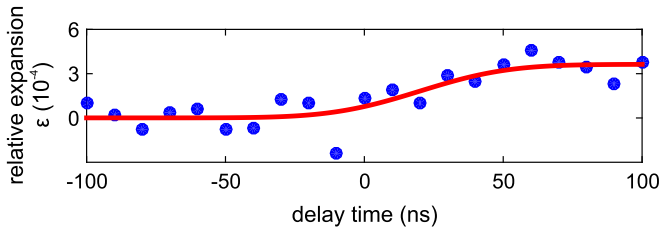

Fig. S2. Representative atomic expansion dynamics of amyloid fibril networks in 10-ns increments.

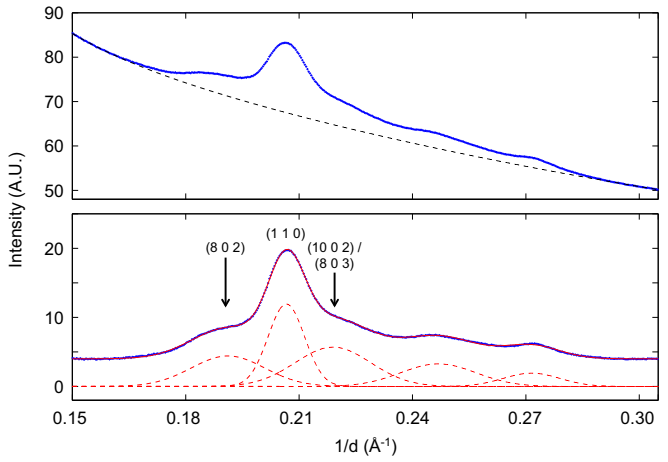

Fig. S3. Angular-integrated 1D diffraction curve of an ensemble of amyloid microcrystals. Also shown are peak assignments, individual fitted profiles of peaks, and background.